Strong Acid Sites Created on Small-Sized Anatase

Hirotoshi NAKABAYASHI,* Noriyoshi KAKUTA,† and Akifumi UENO†
Department of Industrial Chemistry, Kochi College of Technology,
Monobe, Nankoku, Kochi 783
†Department of Materials Science, Toyohashi University of Technology,
Tempaku, Toyohashi, Aichi 441
(Received March 1, 1991)

The acid properties of anatase having different crystalline sizes were estimated by measuring the temperature-programmed desorption (TPD) of ammonia as well as the infrared spectrum of adsorbed pyridine at elevated temperature. The size-controlled anatase was prepared by hydrolysis of the titanium tetraisopropoxide dissolved in propyl alcohol using various amounts of distilled water. The acid properties of the anatase were confirmed to be strongly affected by the crystalline size. Especially, the strength of acid sites was found to remarkably increase with a decrease in the crystalline size. The specific activity and the activation energy for 1-butene isomerization on the anatase also depended on the crystalline size. The generation of strong acid sites on the surface is discussed in terms of the crystalline size.

Acid sites on metal oxides are believed to be ascribed to surface hydroxyl groups or a charge imbalance localized on the surface. Localization of deficient amounts of electrons results from a local imbalance between positive and negative charges of the constituents, and acts as a Lewis acid for catalytic reactions. Since a charge imbalance can be expected by substituting the metal ions with other metal ions possessing different charges, new acid sites could be designed on the surface of doped and/or mixed metal oxides.[1-3] A charge imbalance might emerge, however, even on single-component metal oxides comprising small-sized crystallites, since the electronic properties of tiny metal or metal oxide crystallites have been widely expected to be somewhat different from that of bulk materials.[4] These differences are partially attributed to surface imperfections of crystallographic structures in small-sized crystallites. The typical imperfections in small crystallites are metal or oxygen vacancies, which cause a local charge imbalance.

The idea that new, strong acid sites might be generated on small crystallites has been preliminary demonstrated on TiO_2 by a titration test using several kinds of color indicators.[5] This type titration test, however, sometimes provides us with an ambiguous determination of the acid strength due to a vague change in the color of indicators. The purpose of the present work was to confirm the idea using more reliable methods in measurements of the acid properties, and to understand the generation of strong acid sites in terms of crystalline size.

Experimental

Size-controlled anatase was prepared in the same manner as described elsewhere.[5] In short, 0.025 mol of titanium tetraisopropoxide (Kishida Kagaku Co., 99.9% purity) was dissolved in 50 mL of propyl alcohol, followed by hydrolysis with the desired amounts of distilled water in order to control the size of the resultant TiO_2. The obtained precipitates were dried at 383 K and then calcined at 693 K for 3 h in air. All of the powders, thus produced, were anatase and no trace of rutile was detected by X-ray diffraction measurements, since the phase transformation of anatase to rutile is reported to occur only at temperatures higher than 873 K.[6] The mean sizes of the anatase crystallites were estimated by X-ray line broadening at $2\theta=25.3°$ using the Scherrer equation; 4 kinds of TiO_2 with sizes of around 70, 100, 130, and 170 Å, respectively, were examined. BET surface areas were obtained by N_2 adsorption at 77 K.

The TPD of ammonia on the anatase was carried out using a He purge with a flow rate of 100 mL min^{-1} and a temperature rising rate of 10 K min^{-1}. The sample powder (0.2 g) was first calcined at 693 K in air, and then treated in flowing O_2 at 573 K for 1 h, followed by cooling to room temperature with evacuation. A certain amount of ammonia was iteratively injected into the carrier gas (He), which was introduced over the powder until no more adsorption of ammonia was observed. Pyridine was adsorbed on anatase at 423 K in order to avoid its physical adsorption, followed by evacuation at the desired temperatures. Infrared spectroscopy was employed at room temperature to monitor pyridine still adsorbed on TiO_2, even after evacuation at elevated temperatures.

Isomerization of 1-butene was carried out at temperatures from 413 to 493 K using a closed circulation system made of glass. The sample powder (0.5 g) was first calcined at 693 K in air, and then recalcined at 573 K for 1 h in an O_2 atmosphere, followed by evacuation at room temperature prior to the reaction. The rate constant was estimated, assuming a first-order reaction concerning 1-butene. The initial pressure of 1-butene was always set at 11.8 cmHg (15.72×10^3 Pa) in the present work.

Results

The BET surface areas and the mean crystalline sizes of TiO_2 used in this work are given in Table 1. The highest acid strengths detected by indicators are also given in Table 1. In Fig. 1 are shown the TPD spectra of ammonia on TiO_2 with sizes of about 75, 102, 125, and 162 Å respectively. Three peaks centered around 413, 523, and 663 K are observed in these spectra; the first peak is mainly ascribed to the desorption of ammo-

nia physically adsorbed over TiO_2. Assuming a log-normal distribution for the first peak, the amounts of ammonia chemisorbed were estimated by weighing the other two peaks on the chart. Since ammonia adsorbs on an acid site, the number of acid sites per g and/or m^2 of TiO_2 was calculated (see Fig. 2).

The infrared spectra of pyridine still adsorbed at 423, 523, 623, 673, and 723 K are given in Fig. 3, where the crystalline sizes of TiO_2 used were 82, 125, and 175 Å, respectively. Four absorption peaks were observed at 1610, 1575, 1490, and 1445 cm^{-1} when pyridine was adsorbed on TiO_2 at 423 K. All of the peaks observed

Table 1. BET Surface Areas and the Mean Crystalline Sizes of TiO_2 Studied in This Work.[5] Amounts of Water Employed for the Hydrolysis of $Ti(OC_3H_7)_4$ are Also Given

Sample no.	Water added	Surface area	Crystalline size	Highest Acid strength
	mL	$m^2 g^{-1}$	Å	(H_0)
TiO_2(1)	2000	130	75, 82	−3.0
TiO_2(2)	1000	120	102	−3.0—+1.5
TiO_2(3)	300	105	125	+1.5—+3.3
TiO_2(4)	50	81	162, 175	+3.3—+4.0
TiO_2(5)	Commercial	39	1500—2300	+4.8

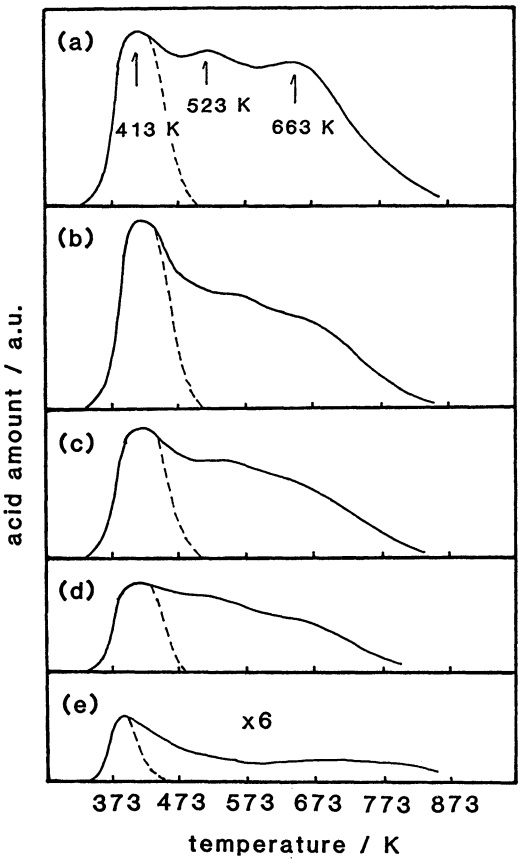

Fig. 1. TPD spectra of ammonia adsorbed on TiO_2 sized 75 Å (a), 102 Å (b), 125 Å (c), and 162 Å (d). For comparison, TPD spectrum of commercial TiO_2 sized around 2000 Å is also depicted.

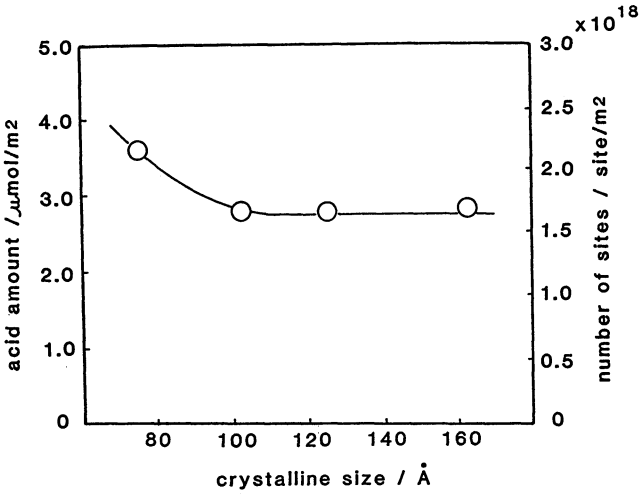

Fig. 2. Numbers of acid sites on TiO_2, given in Fig. 1, expressed in terms of "sites/g" and "sites/m^2".

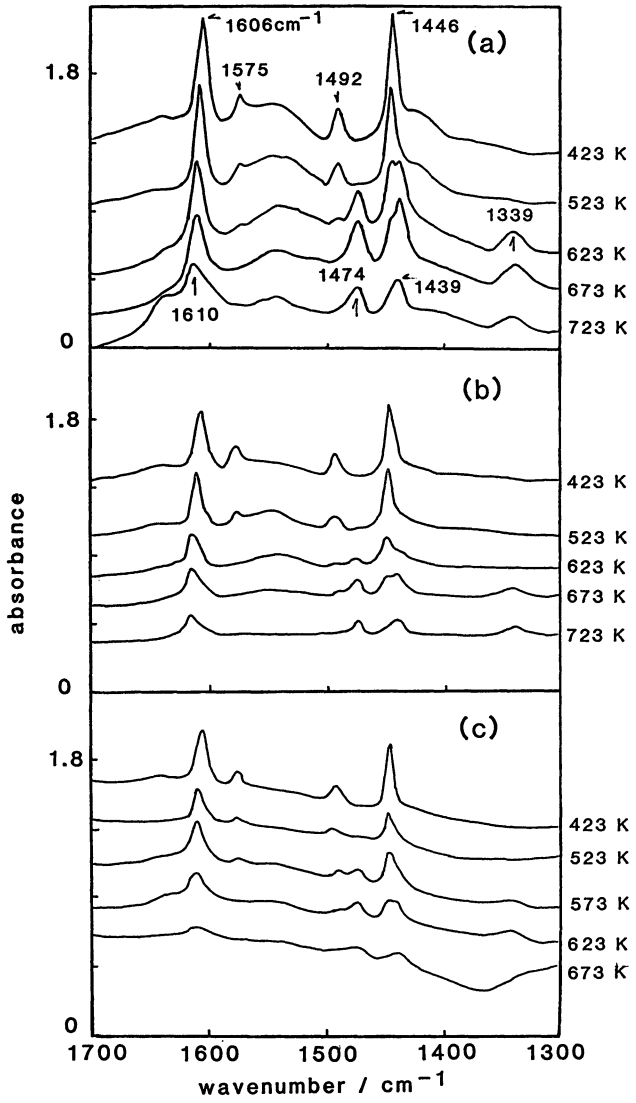

Fig. 3. Infrared spectra of pyridine still adsorbed on TiO_2 at elevated temperatures. TiO_2 studied are sized 82 Å (a), 125 Å (b), and 175 Å (c), respectively.

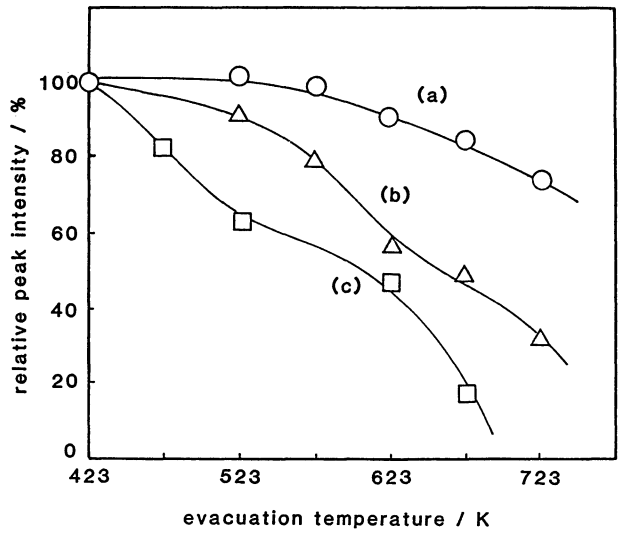

Fig. 4. Decrease in the absorption peak intensity at 1610 cm^{-1} at elevated temperatures. The peak intensities are normalized by the intensity observed after a He purge at 423 K.

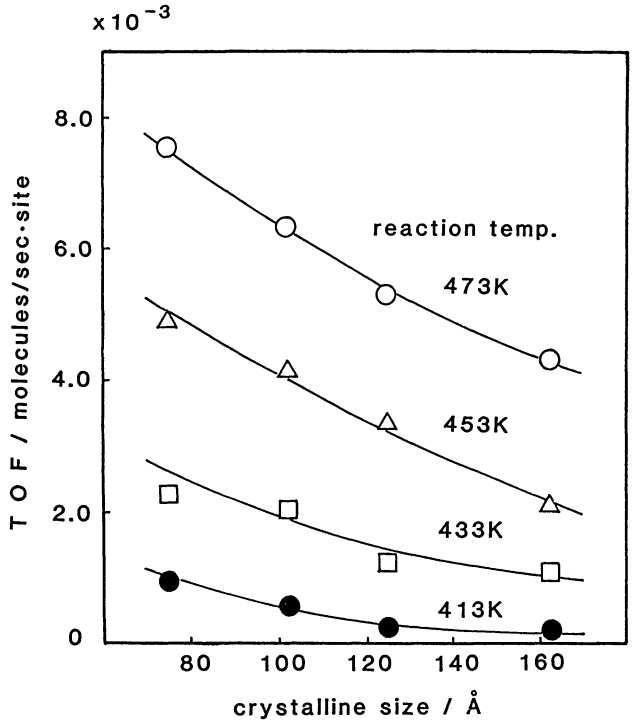

Fig. 5. Change in the turnover frequency of 1-butene isomerization on TiO_2 with the TiO_2 crystalline size.

are ascribed to pyridine adsorbed on the Lewis acid sites,[7] and still remained at temperatures higher than 623 K. Since the area of the absorption peak is proportional to the amounts of pyridine adsorbed, the changes in the peak area at 1610 cm^{-1} with the temperature were monitored for TiO_2 with the crystalline sizes mentioned above. In order to clearly show the difference in these changes, the peak areas were normalized by the peak

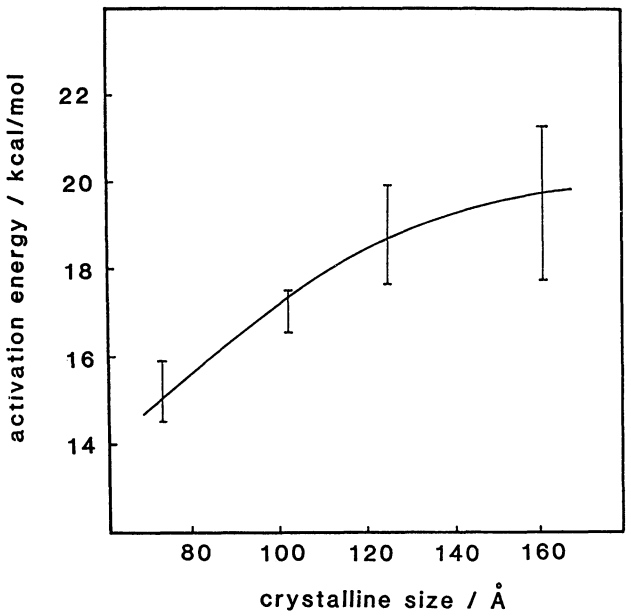

Fig. 6. Change in the activation energy for 1-butene isomerization on TiO_2 with the TiO_2 crystalline size. The activation energies were calculated from the results shown in Fig. 5.

area observed at 423 K for every sample, as shown in Fig. 4.

Since the number of acid sites on TiO_2 was known, the specific activity for 1-butene isomerization on TiO_2 could be expressed in terms of "molecules/sec/site". The obtained results are depicted in Fig. 5 against the crystalline size of TiO_2 used, allowing us to calculate the activation energy on TiO_2 (see Fig. 6).

Discussion

As is obviously shown in Table 1, the crystalline size of TiO_2 decreased as the amount of water used for hydrolysis increased. Although it was not necessarily reproducible to obtain TiO_2 with sizes smaller than 60 Å, which exhibit the highest acid strength of H_0=−5.6, crystallites with sizes of around 70—80 Å with the highest acid strength of H_0=−3.0, could be prepared using more than 2 L of water for hydrolysis. Strong acid sites over the smaller TiO_2 crystallite are also indicated by the TPD of pyridine on TiO_2 with various sizes. In Fig. 3(a) the pyridine adsorbed on TiO_2 with sizes of 82 Å, with H_0(max)=−3.0, is still considerable, even after evacuation at 723 K; on TiO_2 with sizes of around 175 Å (H_0(max)=−8.3), however, only small amounts of pyridine were detected by evacuation at 673 K, as is shown in Fig. 3(c). The fractions of pyridine still adsorbed at various temperatures (drawn in Fig. 4) were determined by monitoring the peak areas at 1610 cm^{-1} and normalizing the areas by the peak areas observed at 423 K. As can clearly be seen in Fig. 4, the fraction of pyridine remaining at elevated temperatures strongly depends on the crystalline size of the

TiO_2 employed; larger amounts of pyridine still remain on smaller TiO_2 crystallites, leading to the conclusion that strong acid sites are created on small-size TiO_2 crystallites. In addition, it would be interesting to discuss the peak shifts which occur in Fig. 3. Although the peak at 1610 cm^{-1} has been reported to shift somewhat toward long wavenumbers with evacuation at elevated temperatures,[8] other peaks observed at 1490 and 1445 cm^{-1} at 423 K were also shown to move to 1475 and 1438 cm^{-1} respectively, after evacuation at 623 K. These shifts could be recognized in all of the samples studied here (see Fig. 3). The new peaks at 1475 and 1438 cm^{-1} were never observed on TiO_2 evacuated at 623 K prior to pyridine adsorption. What happened on the adsorbed pyridine by evacuation at 623 K is yet another problem to be resolved.

The amounts of acid sites over the surface of size-controlled TiO_2 were estimated by measuring the peak areas due to chemisorbed ammonia in ammonia-TPD spectra, assuming one ammonia molecule per one acid site. Although the acid amounts on 1 g of TiO_2 increased with a decrease in the crystalline size, the acid-site density (expressed in terms of "site/m^2") was constant at 1.7×10^{18} sites/m^2 when the crystalline size was larger than 100 Å (see Fig. 2). This indicates that although new acid sites are not created on TiO_2 with sizes larger than 100 Å the acid strength of the sites is modified to be stronger as the crystalline size decreases. Over the surface of TiO_2 with sizes smaller than 100 Å the acid-site densities slightly increased with a decrease in the crystalline size, indicating the generation of new acid sites over the finely divided TiO_2 crystallites. The generation of new acid sites on TiO_2 crystallites with sizes smaller than 100 Å seems to be attributable to metal and/or oxygen ions vacancies which emerged on the surfaces of small TiO_2 crystallites, since these vacancies have been reported to be enhanced in small-size crystallites.[9] In the present work sample powders were reoxidized at 573 K prior to the TPD measurements, suggesting smaller amounts of oxygen ion vacancies on the surface of the TiO_2 used. Consequently, the new acid sites on the finely divided TiO_2 crystallites are tentatively assigned to Ti ion vacancies on the surface.

The strong acid sites over the surface of small TiO_2 crystallites can be elucidated in terms of the electronic properties, which have been widely accepted to be somewhat different from those of bulk-like materials.[4] A blue-shift in the absorption edge of UV-visible spectrum has been reported on tiny TiO_2 particles.[10] This indicates an increase in the bandgap between the conduction and valence band levels of TiO_2 semiconductors. An increase in the bandgap with crystalline size has been estimated by Brus,[11] who calculated the energy of the lowest excited states of various semiconductors. This calculation has been applied to TiO_2 particles,[12] and an increase in the bandgap of small-size TiO_2 has been assigned to an elevation of the conduction band edge. Though the change in the top of the valence band has not been mentioned in this paper, it might be natural to deduce a descent of the valence band edge to expand the bandgap of small TiO_2. A change in the valence band level results in a change in the acid strength of TiO_2 when used as a catalyst, since the positive holes formed in the valence band act as Lewis acid sites during catalysis. Consequently, the descent of the valence band edge in small-sized TiO_2 causes Lewis acid sites with higher acid strengths.

Finally, we tried to relate the acid properties of the finely-divided TiO_2 crystallites to their catalytic performance for the isomerization of 1-butene to *cis*- or *trans*-2-butenes. The product ratio of *cis*/*trans* obtained here was always within the range 1 to 2, suggesting no basic sites, such as Ti^{3+} over TiO_2; this is because the ratio observed on the basic sites has been believed to be much higher than that obtained here.[13] All of the acid sites on the present TiO_2 have been confirmed to be that of the Lewis acid, as discussed above. The isomerization (double bond migration) of 1-butene on Lewis acid sites has been considered to proceed via butenyl cations, which are produced by an elimination of H^- ions from 1-butene adsorbed on the Lewis acid sites.[14] Because the elimination step might be rate-determining regarding doble-bond migration, the catalytic performance of a site strongly depends upon the acid strength. On a stronger acid site, the elimination proceeds faster, leading to a higher turnover frequency on stronger acid sites. The turnover frequencies observed on the present TiO_2 become higher as the crystalline sizes become smaller, as shown in Fig. 5. This coincides well with the results obtained in our preliminary work that strong acid sites emerge on small-size TiO_2 crystallites. From the results shown in Fig. 5, the way in which the activation energies depend upon the size of TiO_2 crystallites is revealed (see Fig. 6).

The generation of both new and strong acid sites on the surfaces of finely-divided TiO_2 crystallites was concluded in the present work; this idea will be extended to the generation of both new and strong acid sites on binary oxides containing tiny TiO_2 crystallites.

References

1) G. L.Thomas, *Ind. Eng. Chem.*, **41**, 2564 (1949).

2) K. Tanabe, "Catalysis, Science and Technology," ed by J. R. Anderson and M. Boudart, Splinger-Verlag, Berlin-Heidelberg-New York (1981), Vol. 2, p. 231; K. Tanabe, "Solid Acids and Base," Kodansha, Tokyo, Academic Press, New York, London (1970).

3) G. Connell and J. A. Dumesic, *J. Catal.*, **102**, 216 (1986); **105**, 285 (1987).

4) J. R. Anderson, "Structure of Metallic Catalysts," Academic Press, New York (1989); M .Boudart, *Adv. Catal.*, **20**, 153 (1969).

5) K. Nishiwaki, N. Kakuta, A. Ueno, and H. Nakabayashi, *J. Catal.*, **118**, 498(1989).

6) R. D. Shannon and J. A. Pask, *J. Am. Chem. Soc.*, **77**, 391 (1965).

7) E. P. Parry, *J. Catal.*, **2**, 371 (1963).
8) M. Primet, P. Pichart, and M. Mathieu, *J. Phys. Chem.*, **75**, 1221 (1971).
9) E. Fujita, *Nihon Kinzoku Gakkaishi,* **30**, 322 (1966); N. F. Mott, *Proc. R. Soc., Ser. A,* **171**, 944 (1939); M. F.Mott, *Trans. Faraday Soc.,* **35**, 1175 (1939); **36**, 472 (1940); **43**, 429 (1947).
10) D. Dounghong, J. Ramsden, and M. Gratzel, *J. Am. Chem. Soc.,* **104**, 2977 (1982); A. Henglein, *Ber. Bunsen-Ges. Phys. Chem.,* **86**, 241 (1982); A. Nojik, F. Williams, M. T. Nenadovic, and O. I. Micic, *J. Phys. Chem.,* **89**, 397 (1985); M. Haase, H. Weller, and A. Henglein, *J. Phys. Chem.,* **92**, 482 (1988).
11) L. E. Brus, *J. Phys. Chem.,* **80**, 4403 (1984); R. Rossetti, S. Nakahara, and E. L. Brus, *J. Phys. Chem.,* **79**, 1986 (1983).
12) C. Korman, D. W. Bahnemann, and M. R. Hoffmann, *J. Phys. Chem.,* **92**, 5196 (1988).
13) Y. Fukuda, H. Hattori, and K. Tanabe, *Bull. Chem. Soc. Jpn.,* **51**, 3150 (1978); M. P. Rosynek and J. S. Fox, *J. Catal.,* **49**, 285 (1977).
14) H. P. Lrftin and E. Hermana, *Proc. Int. Congr. Catal., 3rd, Amsterdam,* **1964** (Put **1965**), No. 2, 1064.